Supplementary material.

Chapter 2: On-farm soybean seed protein and oil prediction using satellite data

Hernandez, C. M., Correndo, A., Kyveryga, P., Prestholt, A., & Ciampitti, I. A. (2023). On-farm soybean seed protein and oil prediction using satellite data. *Computers and Electronics in Agriculture*, *212*, 108096.

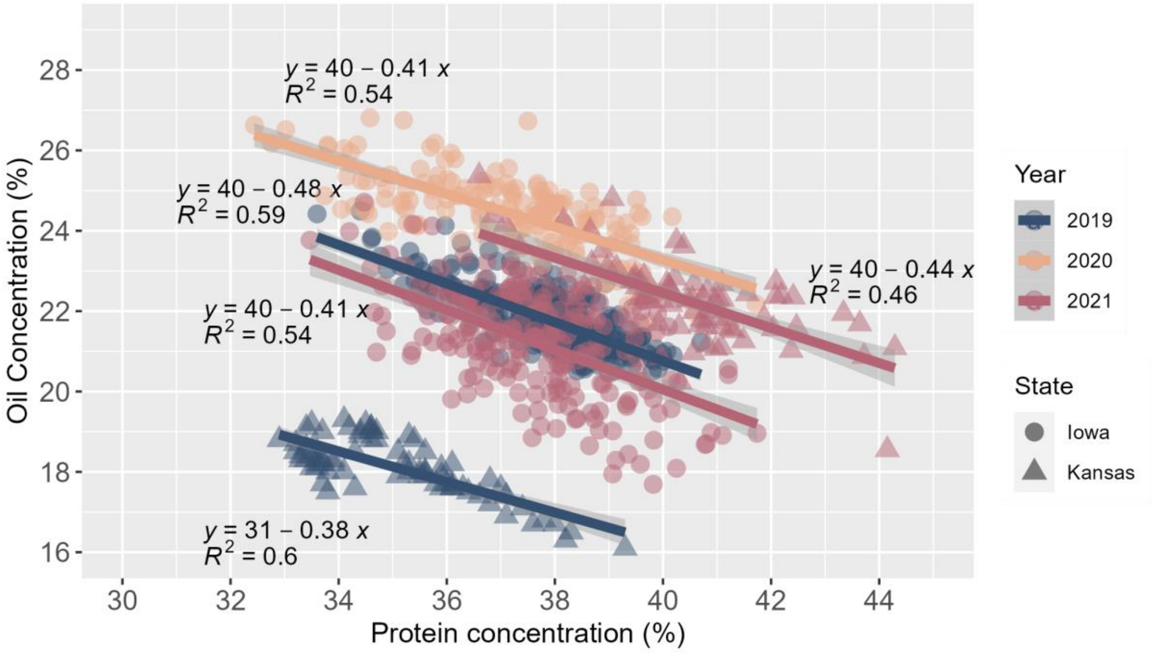

Fig. S1. Relationship between protein and oil concentration in soybean seed samples among years and states.

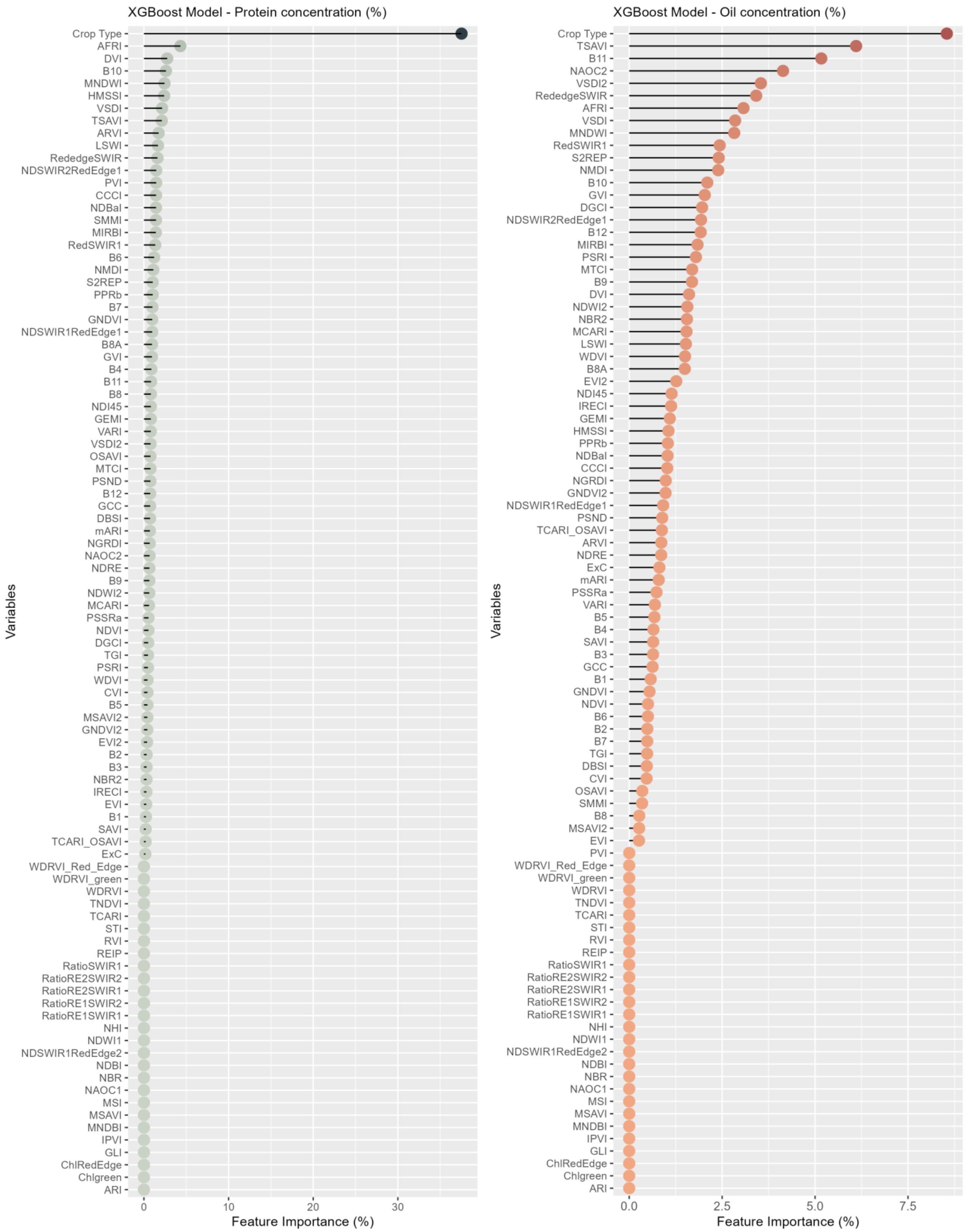

Fig. S2. Detailed graphical description of feature importance assessment for both protein and oil seed concentration models.

Table S1. Accumulated precipitations (mm) and mean temperature (°C) summary from May 1st to September 30th. Values represent mean, minimum and maximum values across site within each State:Year combination.

	Iowa						Kansas					
	Accumulated Precipitation (mm)			Temperature (°C)			Accumulated Precipitation (mm)			Temperature (°C)		
	Mean.	Min	Max.	Mean	Min	Max.	Mean.	Minn	Max.	Mean	Min.	Max.
2019	658	556	779	20.1	19.5	20.5	797	714	930	23.6	23.4	23.7
2020	409	292	582	20.1	19.4	20.4	-	-	-	-	-	-
2021	463	386	546	20.6	20	21	539	515	556	23.7	23.7	23.8

Table S2. Summary with descriptive statistics of Soybean quality seed samples group by fields.

				Protein Concentration (%)			Oil Concentration (%)		
Field ID	Year	State	Crop Type*	Min	Mean	Max	Min	Mean	Max
KS001	2021	Kansas	Full Season	38.88	41.05	43.64	20.96	21.84	23.51
KS002	2021	Kansas	Full Season	38.72	40.64	42.41	21.15	22.05	23.75
KS003	2021	Kansas	Double Crop	39.48	40.58	44.15	18.55	21.60	22.87
KS004	2021	Kansas	Full Season	36.86	40.21	42.47	21.60	22.50	24.38
KS005	2021	Kansas	Double Crop	36.60	39.38	41.87	21.82	23.12	25.37
KS006	2021	Kansas	Double Crop	38.55	40.71	42.08	21.07	22.05	22.82
KS007	2021	Kansas	Double Crop	37.08	38.75	42.09	22.19	23.01	24.16
KS008	2021	Kansas	Double Crop	39.65	41.51	44.29	20.87	22.19	23.62
KS009	2019	Kansas	Double Crop	32.90	33.59	34.30	17.50	18.23	18.80
IA010	2021	Iowa	Full Season	37.11	39.18	41.74	18.68	19.78	21.06
IA011	2021	Iowa	Full Season	35.90	38.69	41.21	20.29	21.99	23.21
IA012	2020	Iowa	Full Season	34.05	36.39	39.16	22.65	24.05	25.23
KS013	2019	Kansas	Double Crop	34.30	36.21	38.00	16.70	17.65	18.50
KS014	2019	Kansas	Double Crop	34.10	35.00	36.10	17.90	18.68	19.30
KS015	2019	Kansas	Double Crop	33.40	36.15	39.30	16.10	17.67	19.20
IA016	2019	Iowa	Full Season	35.64	37.68	39.11	20.51	21.21	22.03
IA017	2019	Iowa	Full Season	37.65	38.53	39.42	20.64	21.23	21.70
IA018	2019	Iowa	Full Season	37.61	38.51	39.05	20.83	21.44	22.02
IA019	2019	Iowa	Full Season	37.63	38.74	39.82	20.76	21.04	21.55
IA020	2019	Iowa	Full Season	36.04	37.91	39.13	20.56	21.41	22.40
IA021	2019	Iowa	Full Season	35.14	36.33	36.96	21.85	22.35	23.12
IA022	2019	Iowa	Full Season	34.40	35.66	37.28	21.70	23.12	24.49
IA023	2019	Iowa	Full Season	33.60	35.95	39.88	21.06	22.92	24.42
IA024	2019	Iowa	Full Season	35.20	36.59	38.03	21.63	22.37	22.71
IA025	2019	Iowa	Full Season	35.82	37.83	39.19	21.37	22.18	23.06

IA026	2019	Iowa	Full Season	35.99	36.97	38.62	21.38	22.13	23.24
IA027	2019	Iowa	Full Season	37.72	39.13	40.19	20.75	21.23	21.87
IA028	2019	Iowa	Full Season	36.98	38.55	39.91	20.51	20.84	21.21
IA029	2019	Iowa	Full Season	36.55	37.97	39.01	20.92	21.42	21.97
IA030	2019	Iowa	Full Season	35.77	38.18	39.80	20.50	21.14	22.34
IA031	2019	Iowa	Full Season	37.94	38.91	39.69	20.97	21.56	22.32
IA032	2019	Iowa	Full Season	35.97	37.74	38.78	21.54	22.52	24.13
IA033	2019	Iowa	Full Season	36.87	38.08	40.07	20.92	21.62	22.35
IA034	2019	Iowa	Full Season	35.85	37.40	38.66	21.15	21.68	22.16
IA035	2019	Iowa	Full Season	35.52	36.66	38.28	21.59	22.28	22.69
IA036	2019	Iowa	Full Season	36.69	38.28	39.61	21.28	21.72	22.58
IA037	2019	Iowa	Full Season	36.08	37.98	39.75	20.92	21.63	23.18
IA038	2019	Iowa	Full Season	37.75	38.02	38.28	21.91	22.17	22.42
IA039	2019	Iowa	Full Season	36.48	38.46	39.79	20.62	21.40	22.55
IA040	2019	Iowa	Full Season	36.74	38.12	40.70	21.23	22.38	23.03
IA041	2019	Iowa	Full Season	36.09	38.01	39.11	21.46	22.31	23.07
IA042	2019	Iowa	Full Season	36.43	37.81	38.58	21.67	22.49	23.25
IA043	2020	Iowa	Full Season	33.74	34.84	36.17	24.48	25.00	25.39
IA044	2020	Iowa	Full Season	32.44	35.08	39.12	24.18	25.57	26.63
IA045	2020	Iowa	Full Season	36.91	37.70	39.40	23.93	24.93	25.47
IA046	2020	Iowa	Full Season	37.68	38.21	39.25	23.04	24.09	24.74
IA047	2020	Iowa	Full Season	36.49	37.71	39.01	23.63	24.56	25.02
IA048	2020	Iowa	Full Season	36.34	37.94	39.61	23.68	24.49	25.24
IA049	2020	Iowa	Full Season	35.79	36.87	38.25	23.73	24.79	25.79
IA050	2020	Iowa	Full Season	35.70	37.86	41.72	22.18	24.90	26.08
IA051	2020	Iowa	Full Season	36.75	39.15	41.22	21.66	23.96	25.15
IA052	2020	Iowa	Full Season	36.61	37.43	39.09	23.07	23.90	24.40
IA053	2020	Iowa	Full Season	34.35	35.77	37.76	24.75	25.61	26.81
IA054	2021	Iowa	Full Season	35.98	37.21	38.51	20.94	21.85	22.89
IA055	2021	Iowa	Full Season	35.50	37.18	39.58	21.55	22.06	22.40
IA056	2021	Iowa	Full Season	34.66	36.12	38.46	20.33	21.66	22.78
IA057	2021	Iowa	Full Season	36.32	36.92	37.78	20.87	21.96	23.39
IA058	2021	Iowa	Full Season	35.80	37.43	38.59	21.00	21.85	22.49
IA059	2021	Iowa	Full Season	35.23	36.26	37.66	20.29	21.65	23.12
IA060	2021	Iowa	Full Season	34.47	36.51	37.82	21.99	23.01	24.71
IA061	2021	Iowa	Full Season	36.06	37.46	38.63	20.66	21.45	22.53
IA062	2021	Iowa	Full Season	33.47	35.79	38.23	21.12	22.40	23.98
IA063	2021	Iowa	Full Season	35.34	37.35	39.07	17.95	20.01	20.90
IA064	2021	Iowa	Full Season	37.58	38.84	40.25	17.69	18.61	19.63
IA065	2021	Iowa	Full Season	35.36	37.57	38.89	19.32	19.97	21.02
IA066	2021	Iowa	Full Season	36.31	38.55	39.72	19.86	20.55	21.41
IA067	2021	Iowa	Full Season	34.80	36.71	37.98	19.93	20.80	21.88
IA068	2021	Iowa	Full Season	34.59	36.29	37.68	20.50	21.84	23.07

IA069	2020	Iowa	Full Season	36.86	38.67	40.57	21.72	23.64	26.73

*Synthetic variable created in 2.2.2

Table S3. Spectral indices singles and compound used spatial information layers.

Index Name	Formula	Sentinel-2 band Assignment	Reference
Green Chromatic Coordinate (GCC)	$\frac{Green}{Blue + Green + Red}$	$\frac{B3}{B2 + B3 + B4}$	(Richardson et al., 2009)
Enhanced vegetation index (EVI)	$2.5 * \frac{Nir - Red}{Nir + (6 * Red) - (7.5 * Blue) + 1}$	$2.5 * \frac{B8 - B4}{B8 + (6 * B4) - (7.5 * B2) + 1}$	(Huete et al., 2002)
Enhanced vegetation index 2 (EVI2)	$2.5 * \frac{NIR - Red}{NIR + 2.4 * Red + 1}$	$2.5 * \frac{B8 - B4}{B8 + 2.4 * B4 + 1}$	(Jiang et al., 2008)
Normalized Difference Vegetation Index (NDVI)	$\frac{NIR - Red}{NIR + Red}$	$\frac{B8 - B4}{B8 + B4}$	(Rouse et al., 1974)
Weight Difference Vegetation Index (WDVI)	$NIR - S * Red ; S = 0.5$	$B8 - S * B4; S = 0.5$	(Clevers, 1989)
Soil Adjusted Vegetation Index (SAVI)	$(\frac{NIR-Red}{NIR+Red+0.25}) * (1 + L) ; L = 0.5$	$\frac{B8 - B4}{B8 + B4 + 0.25}) * (1 + L) ; L = 0.5$	(Huete, 1988)
Modified Soil Adjusted Vegetation Index (MSAVI)	$\left(\frac{(NIR - Red)}{(NIR + Red + 0.25)}\right) * (1 + L) ;$ $L = 1 - 2 * s * NDVI * WDVI ; s = 0.5$	$(\frac{B8 - B4}{B8 + B4 + 0.25}) * (1 + L)$ $L = 1 - 2 * s * NDVI * WDVI ; s = 0.5$	(Qi et al., 1994)
Modified Soil Adjusted Vegetation Index (MSAVI2)	$\frac{\left[2 * NIR + 1 - \sqrt{(2 * NIR + 1)^2 - 8 * (NIR - Red)}\right]}{2}$	$\frac{\left[2 * B8 + 1 - \sqrt{(2 * B8 + 1)^2 - 8 * (B8 - B4)}\right]}{2}$	(Qi et al., 1994)
Infrared percentage vegetation index (IPVI)	$\frac{NIR}{NIR + Red}$	$\frac{B8}{B8 + B4}$	(Crippen, 1990)
Tranformed Normalized Difference Vegetation Index (TNDVI)	$\sqrt{\frac{NIR - Red}{NIR + Red} + 0.5}$	$\sqrt{\frac{B8 - B4}{B8 + B4} + 0.5}$	(Deering, 1975)
Inverted Red-Edge Chloroplyll Index (IRECI)	$\frac{RedEdge3 - Red}{\frac{RedEdge1}{RedEdge2}}$	$\frac{B7 - B4}{\frac{B5}{B6}}$	(Frampton et al., 2013)
Global Environmental Monitoring Index (GEMI)	$\eta * (1 - 0.25 * \eta) - \frac{Red - 0.125}{1 - Red}$ Where $\eta = \frac{[2 * (NIR^2 - Red^2) + 1.5 * NIR + 0.5 * Red]}{(NIR + Red + 5)}$	$\eta * (1 - 0.25 * \eta) - \frac{B4 - 0.125}{1 - B4}$ Where $\eta = \frac{[2 * (B8^2 - Red^2) + 1.5 * B8 + 0.5 * B4]}{(B8 + B4 + 5)}$	(Pinty & Verstraete, 1992)

Normalized Difference Index 45 (NDI45)	$\frac{RedEdge1 - Red}{RedEdge1 + Red}$	$\frac{B5 - B4}{B5 + B4}$	(Delegido et al., 2011)
Perpendicular Vegetation Index (PVI)	$\sqrt{(Gir, s\,Pir)^2 + (Gr, s\,Pr)^2}$	$\sin(a) * B8 - \cos(a) * B4$	(Richardson & Wiegand, 1977)
Difference Vegetation Index (DVI)	$NIR - Red$	$B8 - B4$	(Tucker, 1979)
Pigment Specific Simple Ratio (PSSRa)	$\frac{RedEdge3}{Red}$	$\frac{B7}{B4}$	(Blackburn, 1998)
Transformed Soil Adjusted Vegetation Index (TSAVI)	$\frac{s * (NIR - s * Red - a)}{a * NIR + Red - a * s + X * (1 + s * s)}$ Where a=0.5; s=0.5; X=0.08	$\frac{s * (B8 - s * B4 - a)}{a * B8 + B4 - a * s + X * (1 + s * s)}$ Where a=0.5; s=0.5; X=0.08	(Baret et al., 1989)
Sentinel-2 RedEdge Position (S2REP)	$705 + 35 * \frac{\left(\frac{\rho 783 + \rho 665}{2}\right) - \rho 705}{\rho 740 - \rho 705}$	$705 + 35 * \frac{\left(\frac{B4 + B7}{2}\right) - B5}{B6 - B5}$	(Frampton et al., 2013)
Modified Chlorophyll Absorption Ration Index (MCARI)	$[(RedEdge1 - Red) - 0.2 * (RedEdge1 - Green)] * \frac{RedEdge1}{Red}$	$[(B5 - B4) - 0.2 * (B5 - B3)] * \frac{B5}{B4}$	(Daughtry, 2000)
Triangular Greenness Index (TGI)	$-0.5 * \left(190 * \frac{Red}{Green}\right) - 120 * \left(\frac{Red}{Blue}\right)$	$-0.5 * \left(190 * \frac{B4}{B3}\right) - 120 * \left(\frac{B4}{B2}\right)$	(Hunt et al., 2013)
Normalized Green-Red Difference Index (NGDRI)	$\frac{(Green - Red)}{Green + Red}$	$\frac{B3 - B4}{B3 + B4}$	(Hunt et al., 2005)
Plant Senescence Reflectance Index (PSRI)	$\frac{Red - Blue}{RedEdge2}$	$\frac{B4 - B2}{B6}$	(Merzlyak et al., 1999)
Canopy Chlorophyll Content Index (CCCI)	$\frac{\frac{NIR - RedEdge1}{NIR + RedEdge1}}{\frac{NIR - Red}{NIR + Red}}$	$\frac{\frac{B8 - B5}{B8 + B5}}{\frac{B8 - B4}{B8 + B4}}$	(Long et al., 2009)
Normalized Difference Red-Edge (NDRE)	$\frac{NIR - RedEdge1}{NIR + RedEdge1}$	$\frac{B8 - B5}{B8 + B5}$	(Gitelson & Merzlyak, 1994)
Green Normalized Difference Vegetation Index (GNDVI)	$\frac{NIR - Green}{NIR + Green}$	$\frac{B8 - B3}{B8 + B3}$	(Gitelson et al., 1996)
Green Normalized Difference Vegetation Index (GNDVI2)	$\frac{RedEdge3 - Green}{RedEdge3 + Green}$	$\frac{B7 - B3}{B7 + B3}$	(Gitelson & Merzlyak, 1998)

Ratio Vegetation Index (RVI)	$\frac{NIR}{Red}$	$\frac{B8}{B4}$	(Pearson & Miller, 1972)
Green Vegetation Index (GVI)	$-0.2848 * Blue - 0.2435 * Green - 0.5436 * Red + 0.7243 * NIR + 0.0840 * SWIR1 - 0.1800 * SWIR2$	$-0.2848 * B2 - 0.2435 * B3 - 0.5436 * B4 + 0.7243 * B8 + 0.0840 * B11 - 0.1800 * B12$	(Kauth & Thomas, 1976)
Optimized soil adjusted vegetation index (OSAVI)	$(1 + 0.16) * \frac{(NIR - Red)}{(NIR + Red + 0.16)}$	$(1 + 0.16) * \frac{(B8 - B4)}{(B8 + B4 + 0.16)}$	(Rondeaux et al., 1996)
Transformed Chlorophyll Absorption Reflectance Index (TCARI)	$3 * ((B5 - B4) - 0.2(B5 - B3) * (B5/B4))$	$3 * ((\mathrm{B5} - \mathrm{B4}) - 0.2(\mathrm{B5} - \mathrm{B3}) * (\mathrm{B5}/\mathrm{B4}))$	(Haboudane et al., 2002)
Ratio TCARI / OSAVI (TCARI_OSAVI)	$\frac{3 * ((B5 - B4) - 0.2(B5 - B3) * (B5/B4))}{(1 + 0.16) * \frac{(NIR - Red)}{(NIR + Red + 0.16)}}$	$\frac{3 * ((\mathrm{B5} - \mathrm{B4}) - 0.2(\mathrm{B5} - \mathrm{B3}) * (\mathrm{B5}/\mathrm{B4}))}{(1 + 0.16) * \frac{(B8 - B4)}{(B8 + B4 + 0.16)}}$	(Haboudane et al., 2002)
Green Chlorophyll Vegetation Index (GCVI)	$\frac{NIR}{Green} - 1$	$\frac{B8}{B3} - 1$	(Gitelson et al., 1996)
Red-Edge Chlorophyll Vegetation Index (ChlRedEdge)	$\frac{NIR}{RedEdge1} - 1$	$\frac{B8}{B5} - 1$	(Gitelson et al., 2003)
MERIS Terrestrial Chlorophyll Index (MTCI)	$\frac{RedEdge2 - RedEdge1}{RedEdge1 - Red}$	$\frac{B6 - B5}{B5 - B4}$	(Dash & Curran, 2004)
Red-Edge Inflection Point (REIP)	$700 + 40 * \frac{\left(\frac{Red + RedEdge3}{2}\right) - RedEdge1}{RedEdge2 - RedEdge1}$	$700 + 40 * \frac{\left(\frac{B4 + B7}{2}\right) - B5}{B6 - B5}$	(Herrmann et al., 2011)
Atmospheric Resistant Vegetation Index (ARVI)	$\frac{NIR - 2 * Red - Blue}{NIR + 2 * Red - Blue}$	$\frac{B8 - 2 * B4 - B2}{B8 + 2 * B4 - B2}$	(Kaufman & Tanre, 1992)
Chlorophyll Vegetation Index (CVI)	$\frac{(\frac{NIR}{Green})}{(\frac{Green}{Red})}$	$\frac{(\frac{B8}{B3})}{(\frac{B3}{B4})}$	(Vincini et al., 2008)
Wide Dynamic Range Vegetation Index (WDRVI)	$\frac{(\alpha * NIR - Red)}{(\alpha * NIR + Red)}; \alpha = 0.1$	$\frac{(\alpha * B8 - B4)}{(\alpha * B8 + B4)}; \alpha = 0.1$	(Gitelson, 2004)
Green Wide Dynamic Range Vegetation Index (Green WDRVI)	$\frac{(\alpha * NIR - Green)}{(\alpha * NIR + Green)}; \alpha = 0.1$	$\frac{(\alpha * B8 - B3)}{(\alpha * B8 + B3)}; \alpha = 0.1$	(Peng & Gitelson, 2011)
Red Edge Wide Dynamic Range Vegetation Index Red Edge	$\frac{(\alpha * NIR - RedEdge1)}{(\alpha * NIR + RedEdge1)}; \alpha = 0.1$	$\frac{(\alpha * B8 - B5)}{(\alpha * B8 + B5)}; \alpha = 0.1$	(Peng & Gitelson, 2011)

(Red Edge WDRVI)			
Heavy Metal Stress Sensitive Index (HMSSI)	$\frac{\frac{NIR}{RedEdge1} - 1}{\frac{Red - Blue}{RedEdge2}}$	$\frac{\frac{B8}{B5} - 1}{\frac{B4 - B2}{B6}}$	(Silva Junior et al., 2020)
Excess Green Index (ExG)	$2 * Green - Red - Blue$	$2 * B3 - B4 - B2$	(Woebbecke et al., 1995)
Plant Pigment Ratio (PPRb)	$\frac{Green - Blue}{Green + Blue}$	$\frac{B3 - B2}{B3 + B2}$	(Metternicht, 2003)
Visible Atmospherically Resistant Index (VARI)	$\frac{Green - Red}{Green + Red - Blue}$	$\frac{B3 - B4}{B3 + B4 - B2}$	(Gitelson et al., 2002)
Green Leaf Index (GLI)	$\frac{2 * Green - Red - Blue}{2 * Green + Red + Blue}$	$\frac{2 * B3 - B4 - B2}{2 * B3 + B4 + B2}$	(Louhaichi et al., 2001)
Anthocyanin Reflectance Index (ARI)	$\frac{1}{Green} - \frac{1}{RedEdge1}$	$\frac{1}{B3} - \frac{1}{B5}$	(Gitelson et al., 2009)
Dark Green Color Index (DGCI)	$\frac{\left[\frac{H-60}{60}\right] + (1-S) + (1+B)}{3}$ $H = \begin{cases} \text{IF}(\max(R,G,B) = R)\ THEN\ 60 * \left\{\frac{G-R}{\max(R,G,B) - \min(R,G,B)}\right\} \\ \text{IF}(\max(R,G,B) = G)\ THEN\ 60 * \left\{\frac{B-R}{\max(R,G,B) - \min(R,G,B)}\right\} \\ \text{IF}(\max(R,G,B) = B)\ THEN\ 60 * \left\{\frac{R-G}{\max(R,G,B) - \min(R,G,B)}\right\} \end{cases}$ B = max(r, g, b) $S = \frac{(\max(R,G,B) - \min(R,G,B))}{\max(R,G,B)}$ R = Red / (Red+Green+Blue) G = Green / (Red+Green+Blue) B = Blue / (Red+Green+Blue)	$\frac{\left[\frac{H-60}{60}\right] + (1-S) + (1+B)}{3}$ $H = \begin{cases} \text{IF}(\max(R,G,B) = R)\ THEN\ 60 * \left\{\frac{G-R}{\max(R,G,B) - \min(R,G,B)}\right\} \\ \text{IF}(\max(R,G,B) = G)\ THEN\ 60 * \left\{\frac{B-R}{\max(R,G,B) - \min(R,G,B)}\right\} \\ \text{IF}(\max(R,G,B) = B)\ THEN\ 60 * \left\{\frac{R-G}{\max(R,G,B) - \min(R,G,B)}\right\} \end{cases}$ B = max(R, G, B) $S = \frac{(\max(R,G,B) - \min(R,G,B))}{\max(R,G,B)}$ R = B4 / (B4+B3+B2) G = B3 / (B4+B3+B2) B = B2 / (B4+B3+B2)	(Karcher & Richardson, 2003)
Modified Anthocyanin Reflectance Index (mARI)	$\left(\frac{1}{Green}\right) - \left(\frac{1}{RedEdge1}\right) * RedEdge3$	$\left(\frac{1}{B3}\right) - \left(\frac{1}{B5}\right) * B7$	(Gitelson et al., 2009)
Pigment-specific Normalized Difference Index (PSND)	$\frac{NIR - Blue}{NIR + Blue}$	$\frac{B8 + B2}{B8 + B2}$	(Blackburn, 1998)
Normalized Area Over Reflectance Curve 1 (NAOC1)	$\frac{1}{2} * (1 - \frac{RedEdge3}{Red})$	$\frac{1}{2} * (1 - \frac{B7}{B4})$	(Parida et al., 2022)
Normalized Area Over Reflectance Curve 2 (NAOC2)	$1 - \frac{(Red * 40) + (RedEdge1 * 35) + (RedEdge2 * 43)}{(RedEdge3 * 118)}$	$1 - \frac{(B4 * 40) + (B5 * 35) + (B6 * 43)}{(B7 * 118)}$	(Cisneros et al., 2020; Delegido et al., 2010)
Normalized Difference Water Index 1 (NDWI1)	$\frac{Green - NIR}{Green + NIR}$	$\frac{B3 - B8}{B3 + B8}$	(Mc Feeters, 1996)

Normalized Difference Water Index 2 (NDWI2)	$\frac{NIR - SWIR2}{NIR + SWIR2}$	$\frac{B8 - B12}{B8 + B12}$	(Gao, 1996)
Aerosol Free Vegetation Index (D)	$\frac{NIRn - 0.66 * SWIR1}{NIRn + 0.66 * SWIR1}$	$\frac{B8A - 0.66 * B11}{B8A + 0.66 * B11}$	(Karnieli et al., 2001)
Dry Bare Soil Index (DBSI)	$\frac{SWIR1 - Green}{SWIR1 + Green - NDVI}$	$\frac{B11 - B3}{B11 + B3 - NDVI}$	(Rasul et al., 2018)
Land Surface Water Index (LSWI)	$\frac{NIR - SWIR1}{NIR + SWIR1}$	$\frac{B8 - B11}{B8 + B11}$	(Xiao et al., 2006)
Mid Infrared Burned Index (MIRBI)	$10 * SWIR2 - 9.8 * SWIR1 + 2$	$10 * B12 - 9.8 * B11 + 2$	(Trigg & Flasse, 2001)
Modified Normalized Difference Build-up Index (MNDBI)	$\frac{SWIR2 - NIR}{SWIR2 + NIR}$	$\frac{B12 - B8}{B12 + B8}$	(Shingare et al., 2014)
Modified Normalized Difference Water Index (MNDWI)	$\frac{Green - SWIR1}{Green + SWIR1}$	$\frac{B3 - B11}{B3 + B11}$	(Xu, 2008)
Normalized Burn Ratio (NBR)	$\frac{SWIR2 - NIRn}{SWIR2 + NIRn}$	$\frac{B12 - B8A}{B12 + B8A}$	(García & Caselles, 1991)
Normalized Burn Ratio 2 (NBR2)	$\frac{SWIR1 - SWIR2}{SWIR1 + SWIR2}$	$\frac{B11 - B12}{B11 + B12}$	(Key & Benson, 2005)
Normalized Difference Bareness Index (NDBaI)	$\frac{RedEdge2 - SWIR1}{RedEdge2 + SWIR1}$	$\frac{B6 - B11}{B6 + B11}$	(Zhao & Chen, 2005)
Normalized Differences Build-Up Index (NDBI)	$\frac{SWIR1 - NIR}{SWIR1 + NIR}$	$\frac{B11 - B8}{B11 + B8}$	(Zha et al., 2003)
Soil Tillage Index (STI)	$\frac{SWIR1}{SWIR2}$	$\frac{B11}{B12}$	(Deventer et al., 1997)
Red and SWIR band Difference (RedSWIR1)	$\frac{SWIR1}{NIR}$	$\frac{B11}{B8}$	(Jacques et al., 2014)
Visible and Shortwave Infrared Drought Index (VSDI)	$\frac{SWIR1 - NIRn}{SWIR1 + NIRn}$	$\frac{B11 - B8A}{B11 + B8A}$	(Zhang et al., 2013)
Moisture Stress Index (MSI)	$\frac{SWIR1}{NIRn}$	$\frac{B11}{B8A}$	(Rock et al., 1985)

Normalized Difference Red Edge and SWIR (RedEdgeSWIR)	$\frac{RedEdge2 - SWIR2}{RedEdge2 + SWIR2}$	$\frac{B6 - B12}{B6 + B12}$	(Rondeaux et al., 1996)
Normalized Humedity Index (NHI)	$\frac{SWIR1 - Green}{SWIR + Green}$	$\frac{B11 - B3}{B11 + B3}$	(Lacaux et al., 2007)
Normalized Multi-band Drought Index (NMDI)	$\frac{NIR - SWIR1 - SWIR2}{NIR + SWIR1 + SWIR2}$	$\frac{B8 - B11 - B12}{B8 + B11 + B12}$	(Wang & Qu, 2007)
Soil Moisture Monitoring Index (SMMI)	$\frac{\sqrt{NIRn^2 + SWIR1^2}}{\sqrt{2}}$	$\frac{\sqrt{B8A^2 + B11^2}}{\sqrt{2}}$	(Chen et al., 2020)
Visible and Shortwave Infrared Drought Index 2 (VSDI2)	$1 - (SWIR2 + Red - 2 * Blue)$	$1 - (B12 + B4 - 2 * B2)$	(Hazaymeh & Hassan, 2017)
NDSWIR2RedEdge1	$\frac{SWIR2 - RedEdge1}{SWIR2 + RedEdge1}$	$\frac{B12 - B5}{B12 + B5}$	Proposed by the author
NDSWIR1RedEdge1	$\frac{SWIR1 - RedEdge1}{SWIR1 + RedEdge1}$	$\frac{B11 - B5}{B11 + B5}$	Proposed by the author
NDSWIR1RedEdge2	$\frac{SWIR1 - RedEdge2}{SWIR1 + RedEdge2}$	$\frac{B11 - B6}{B11 + B6}$	Proposed by the author
Ratio SWIR1	$\frac{SWIR2}{SWIR1}$	$\frac{B12}{B11}$	(Guerschman et al., 2009)
Ratio RE1 and SWIR2	$\frac{RedEdge1}{SWIR2}$	$\frac{B5}{B12}$	Proposed by the author
Ratio RE1 and SWIR1	$\frac{RedEdge1}{SWIR1}$	$\frac{B5}{B11}$	Proposed by the author
Ratio RE2 and SWIR1	$\frac{RedEdge2}{SWIR1}$	$\frac{B6}{B11}$	Proposed by the author
Ratio RE2 and SWIR2	$\frac{RedEdge2}{SWIR2}$	$\frac{B6}{B12}$	Proposed by the author

Table S4. Hyper-parameters corresponding to each machine learning model tested for prediction of protein and oil concentration.

Variable	Model	Hyperparameter	Range tried	Optimized value
Protein Concentration (%)	ElasticNet	max_iter	1, 5, 10,50	10
		alpha	0.0001, 0.001, 0.01, 0.1, 1, 10, 100	0.0001

		l1_ratio	0., 0.05, 0.1, 0.15, 0.2, 0.25, 0.3, 0.35, 0.4, 0.45, 0.5, 0.55, 0.6, 0.65, 0.7, 0.75, 0.8, 0.85, 0.9, 0.95	0
	XGBoost	max_depth	3, 5, 15	5
		learning_rate	0.5, 0.1, 0.05, 0.01	0.1
		n_estimators	5, 100,500,1500	500
	LightGBM	learning_rate	0.01, 0.05, 0.1, 0.9	0.1
		n_estimators	50, 100, 500	100
		max_depth	5, 15, 50	5
	Random Forest	max_depth	5, 15	15
		max_features	auto, sqrt, log2	auto
		n_estimators	5, 50, 100	100
	CatBoost	depth	5,50,150	5
		n_estimators	10,250,500,1000	1000
		learning_rate	0.01, 0.1	0.01
Oil Concentration (%)	ElasticNet	max_iter	1, 5, 10,50	50
		alpha	0.0001, 0.001, 0.01, 0.1, 1, 10, 100	0.01
		l1_ratio	0., 0.05, 0.1, 0.15, 0.2, 0.25, 0.3, 0.35, 0.4, 0.45, 0.5, 0.55, 0.6, 0.65, 0.7, 0.75, 0.8, 0.85, 0.9, 0.95	0.1
	XGBoost	max_depth	3, 5, 15	5
		learning_rate	0.5, 0.1, 0.05, 0.01	0.05
		n_estimators	5, 100,500,1500	1500
	LightGBM	learning_rate	0.01, 0.05, 0.1, 0.9	0.05
		n_estimators	50, 100, 500	500
		max_depth	5, 15, 50	15
	Random Forest	max_depth	5, 15	15
		max_features	auto, sqrt, log2	Auto
		n_estimators	5, 100, 250	250
	CatBoost	depth	5,50	5
		n_estimators	10,100,500,3000	3000
		learning_rate	0.01, 0.1	0.1

Table S5. Predictive performance metrics and indices used for model comparison and prediction quality evaluation.

Metrics	Definition	Formulation
R^2	Coefficient of determination	$R^2 = \frac{S^2{}_{PO}}{S^2{}_{P}\, P^2{}_{O}}$

CCC	Concordance correlation coefficient	$CCC = r * X_a$
RMSE	Root Mean Squared Error	$RMSE = \sqrt{\frac{1}{n}\sum(P_i - O_i)^2}$
RRMSE	Relative Root Mean Squared Error	$RRMSE = \frac{\sqrt{\frac{1}{n}\sum(P_i - O_i)^2}}{\bar{O}}$
MBE	Mean Bias Error	$MBE = \frac{1}{n}\sum(O_i - P_i) = \bar{O} - \bar{P}$
PLA	Percentage Lack of Accuracy	$PLA = 100\frac{(\bar{O} - \bar{P})^2 + (S_O - S_P)^2}{\frac{1}{n}\sum(P_i - O_i)^2}$
PLP	Percentage Lack of Precision	$PLP = 100\frac{2S_oS_P(1-r)}{\frac{1}{n}\sum(P_i - O_i)^2}$
KGE	Kling-Gupta Model Efficiency	$KGE = 1 - \sqrt{(r-1)^2 + (\frac{S_p}{S_O} - 1)^2 + (\frac{\bar{P}}{\bar{O}} - 1)^2}$

Where Oi; observed; Pi; predicted, S: variance; r: Pearson correlation coefficient; X_a: Accuracy coefficient; n: sample size; $\bar{O}$: mean of observed; $\bar{P}$: mean of predicted.

Table S6. Predictive performance metrics of the different candidate models for both Protein and Oil concentration using training subset.

		Predicting performance metrics							
	Models	R^2	CCC	RMSE	RRMSE (%)	MBE	PLA	PLP	KGE
Protein concentration (%)	ElasticNet	0.40	0.57	1.33	3.50	<0.01	24	76	0.47
	XGBoost	1.00	1.00	0.00	0.00	<0.01	14	86	0.99
	LightGBM	0.93	0.95	0.48	1.27	<0.01	28	72	0.84
	Random Forest	0.94	0.95	0.47	1.24	<0.01	35	64	0.83
	CatBoost	0.82	0.87	0.77	2.02	<0.01	32	68	0.73
	Ensemble	0.90	0.91	0.62	1,63	<0.01	39	61	0.77
Oil concentration (%)	ElasticNet	0.34	0.50	1.11	5.04	<0.01	29	71	0.39
	XGBoost	0.99	0.99	<0.01	<0.01	<0.01	12	88	0.99
	LightGBM	0.99	0.99	0.08	0.38	<0.01	9	91	0.98
	Random Forest	0.94	0.95	0.39	1.78	<0.01	45	55	0.80
	CatBoost	0.99	0.99	<0.01	<0.01	<0.01	6	94	0.99
	Ensemble	0.94	0.93	0.42	1.93	<0.01	58	42	0.76

Where R^2: Coefficient of determination; CCC: Concordance correlation coefficient; RMSE: Root Mean Squared Error; RRMSE: Relative Root Mean Squared Error; MBE: Mean Bias Error; PLA: Percentage Lack of Accuracy; PLP: Percentage Lack of Precision; KGE: Kling-Gupta Model Efficiency.

References

Baret, F., Guyot, G., & Major, D. J. (1989). TSAVI: A Vegetation Index Which Minimizes Soil Brightness Effects on LAI And APAR Estimation. *12th Canadian Symposium on Remote Sensing Geoscience and Remote Sensing Symposium*, *3*, 1355–1358. https://doi.org/10.1109/IGARSS.1989.576128

Blackburn, G. A. (1998). Quantifying Chlorophylls and Caroteniods at Leaf and Canopy Scales. *Remote Sensing of Environment*, *66*(3), 273–285. https://doi.org/10.1016/S0034-4257(98)00059-5

Chen, Y., Qiu, Y., Zhang, Z., Zhang, J., Chen, C., Han, J., & Liu, D. (2020). Estimating salt content of vegetated soil at different depths with Sentinel-2 data. *PeerJ*, *8*, e10585. https://doi.org/10.7717/peerj.10585

Cisneros, A., Fiorio, P., Menezes, P., Pasqualotto, N., Van Wittenberghe, S., Bayma, G., & Furlan Nogueira, S. (2020). Mapping Productivity and Essential Biophysical Parameters of Cultivated Tropical Grasslands from Sentinel-2 Imagery. *Agronomy*, *10*(5), 711. https://doi.org/10.3390/agronomy10050711

Clevers, J. (1989). Application of a weighted infrared-red vegetation index for estimating leaf area index by correcting for soil moisture. *Remote Sensing of Environment*, *29*(1), 25–37.

Crippen, R. E. (1990). Calculating the vegetation index faster. *Remote Sensing of Environment*, *34*(1), 71–73.

Dash, J., & Curran, P. J. (2004). The MERIS terrestrial chlorophyll index. *International Journal of Remote Sensing*, *25*(23), 5403–5413. https://doi.org/10.1080/0143116042000274015

Daughtry, C. (2000). Estimating Corn Leaf Chlorophyll Concentration from Leaf and Canopy Reflectance. *Remote Sensing of Environment*, *74*(2), 229–239. https://doi.org/10.1016/S0034-4257(00)00113-9

Deering, D. (1975). *Measuring" forage production" of grazing units from Landsat MSS data*. 1169–1198.

Delegido, J., Alonso, L., González, G., & Moreno, J. (2010). Estimating chlorophyll content of crops from hyperspectral data using a normalized area over reflectance curve (NAOC). *International Journal of Applied Earth Observation and Geoinformation*, *12*, 165–174.

Delegido, J., Verrelst, J., Alonso, L., & Moreno, J. (2011). Evaluation of sentinel-2 red-edge bands for empirical estimation of green LAI and chlorophyll content. *Sensors*, *11*(7), 7063–7081.

Deventer, van, Ward, A., Gowda, P., & Lyon, J. (1997). Using Thematic Mapper Data to Identify Contrasting Soil Plains and Tillage Practices. *Photogrammetric Engineering and Remote Sensing*, *63*, 87–93.

Frampton, W. J., Dash, J., Watmough, G., & Milton, E. J. (2013). Evaluating the capabilities of Sentinel-2 for quantitative estimation of biophysical variables in vegetation. *ISPRS Journal of Photogrammetry and Remote Sensing*, *82*, 83–92. https://doi.org/10.1016/j.isprsjprs.2013.04.007

Gao, B. (1996). NDWI—A normalized difference water index for remote sensing of vegetation liquid water from space. *Remote Sensing of Environment*, *58*(3), 257–266. https://doi.org/10.1016/S0034-4257(96)00067-3

García, M. J. L., & Caselles, V. (1991). Mapping burns and natural reforestation using thematic Mapper data. *Geocarto International*, *6*(1), 31–37. https://doi.org/10.1080/10106049109354290

Gitelson, A. A. (2004). Wide Dynamic Range Vegetation Index for Remote Quantification of Biophysical Characteristics of Vegetation. *Journal of Plant Physiology*, *161*(2), 165–173. https://doi.org/10.1078/0176-1617-01176

Gitelson, A. A., Chivkunova, O. B., & Merzlyak, M. N. (2009). Nondestructive estimation of anthocyanins and chlorophylls in anthocyanic leaves. *American Journal of Botany*, *96*(10), 1861–1868. https://doi.org/10.3732/ajb.0800395

Gitelson, A. A., Gritz †, Y., & Merzlyak, M. N. (2003). Relationships between leaf chlorophyll content and spectral reflectance and algorithms for non-destructive chlorophyll assessment in higher plant leaves. *Journal of Plant Physiology*, *160*(3), 271–282. https://doi.org/10.1078/0176-1617-00887

Gitelson, A. A., Kaufman, Y. J., & Merzlyak, M. N. (1996). Use of a green channel in remote sensing of global vegetation from EOS-MODIS. *Remote Sensing of Environment*, *58*(3), 289–298.

Gitelson, A. A., Kaufman, Y. J., Stark, R., & Rundquist, D. (2002). Novel algorithms for remote estimation of vegetation fraction. *Remote Sensing of Environment*, *80*(1), 76–87. https://doi.org/10.1016/S0034-4257(01)00289-9

Gitelson, A. A., & Merzlyak, M. N. (1998). Remote sensing of chlorophyll concentration in higher plant leaves. *Advances in Space Research*, *22*(5), 689–692. https://doi.org/10.1016/S0273-1177(97)01133-2

Gitelson, A., & Merzlyak, M. N. (1994). Spectral Reflectance Changes Associated with Autumn Senescence of Aesculus hippocastanum L. and Acer platanoides L. Leaves. Spectral Features and Relation to Chlorophyll Estimation. *Journal of Plant Physiology*, *143*(3), 286–292. https://doi.org/10.1016/S0176-1617(11)81633-0

Guerschman, J. P., Hill, M. J., Renzullo, L. J., Barrett, D. J., Marks, A. S., & Botha, E. J. (2009). Estimating fractional cover of photosynthetic vegetation, non-photosynthetic vegetation and bare soil in the Australian tropical savanna region upscaling the EO-1 Hyperion and MODIS sensors. *Remote Sensing of Environment*, *113*(5), 928–945. https://doi.org/10.1016/j.rse.2009.01.006

Haboudane, D., Miller, J. R., Tremblay, N., Zarco-Tejada, P. J., & Dextraze, L. (2002). Integrated narrow-band vegetation indices for prediction of crop chlorophyll content for application to precision agriculture. *Remote Sensing of Environment*, *81*(2–3), 416–426. https://doi.org/10.1016/S0034-4257(02)00018-4

Hazaymeh, K., & Hassan, Q. K. (2017). A remote sensing-based agricultural drought indicator and its implementation over a semi-arid region, Jordan. *Journal of Arid Land*, *9*(3), 319–330. https://doi.org/10.1007/s40333-017-0014-6

Herrmann, I., Pimstein, A., Karnieli, A., Cohen, Y., Alchanatis, V., & Bonfil, D. J. (2011). LAI assessment of wheat and potato crops by VENμS and Sentinel-2 bands. *Remote Sensing of Environment*, *115*(8), 2141–2151. https://doi.org/10.1016/j.rse.2011.04.018

Huete, A., Didan, K., Miura, T., Rodriguez, E. P., Gao, X., & Ferreira, L. G. (2002). Overview of the radiometric and biophysical performance of the MODIS vegetation indices. *Remote Sensing of Environment*, *83*(1–2), 195–213.

Huete, A. R. (1988). A soil-adjusted vegetation index (SAVI). *Remote Sensing of Environment*, *25*(3), 295–309.

Hunt, E. R., Cavigelli, M., Daughtry, C. S. T., Mcmurtrey, J. E., & Walthall, C. L. (2005). Evaluation of Digital Photography from Model Aircraft for Remote Sensing of Crop Biomass and Nitrogen Status. *Precision Agriculture*, *6*(4), 359–378. https://doi.org/10.1007/s11119-005-2324-5

Hunt, E. R., Doraiswamy, P. C., McMurtrey, J. E., Daughtry, C. S. T., Perry, E. M., & Akhmedov, B. (2013). A visible band index for remote sensing leaf chlorophyll content at the canopy scale. *International Journal of Applied Earth Observation and Geoinformation*, *21*, 103–112. https://doi.org/10.1016/j.jag.2012.07.020

Jacques, D. C., Kergoat, L., Hiernaux, P., Mougin, E., & Defourny, P. (2014). Monitoring dry vegetation masses in semi-arid areas with MODIS SWIR bands. *Remote Sensing of Environment*, *153*, 40–49. https://doi.org/10.1016/j.rse.2014.07.027

Jiang, Z., Huete, A. R., Didan, K., & Miura, T. (2008). Development of a two-band enhanced vegetation index without a blue band. *Remote Sensing of Environment*, *112*(10), 3833–3845.

Karcher, D. E., & Richardson, M. D. (2003). Quantifying Turfgrass Color Using Digital Image Analysis. *Crop Science*, *43*(3), 943–951. https://doi.org/10.2135/cropsci2003.9430

Karnieli, A., Kaufman, Y. J., Remer, L., & Wald, A. (2001). AFRI — aerosol free vegetation index. *Remote Sensing of Environment*, *77*(1), 10–21. https://doi.org/10.1016/S0034-4257(01)00190-0

Kaufman, Y. J., & Tanre, D. (1992). Atmospherically resistant vegetation index (ARVI) for EOS-MODIS. *IEEE Transactions on Geoscience and Remote Sensing*, *30*(2), 261–270. https://doi.org/10.1109/36.134076

Kauth, R. J., & Thomas, G. (1976). *The tasselled cap—A graphic description of the spectral-temporal development of agricultural crops as seen by Landsat*. 159.

Key, C., & Benson, N. (2005). *Landscape Assessment (LA) Sampling and Analysis Methods* (p. LA 1-51).

Lacaux, J. P., Tourre, Y. M., Vignolles, C., Ndione, J. A., & Lafaye, M. (2007). Classification of ponds from high-spatial resolution remote sensing: Application to Rift Valley Fever epidemics in Senegal. *Remote Sensing of Environment*, *106*(1), 66–74. https://doi.org/10.1016/j.rse.2006.07.012

Long, D. S., Eitel, J. U. H., & Huggins, D. R. (2009). Assessing Nitrogen Status of Dryland Wheat Using the Canopy Chlorophyll Content Index. *Crop Management*, *8*(1), 1–8. https://doi.org/10.1094/CM-2009-1211-01-RS

Louhaichi, M., Borman, M. M., & Johnson, D. E. (2001). Spatially Located Platform and Aerial Photography for Documentation of Grazing Impacts on Wheat. *Geocarto International*, *16*(1), 65–70. https://doi.org/10.1080/10106040108542184

M. Woebbecke, D., E. Meyer, G., Von Bargen, K., & A. Mortensen, D. (1995). Color Indices for Weed Identification Under Various Soil, Residue, and Lighting Conditions. *Transactions of the ASAE*, *38*(1), 259–269. https://doi.org/10.13031/2013.27838

McFEETERS, S. K. (1996). The use of the Normalized Difference Water Index (NDWI) in the delineation of open water features. *International Journal of Remote Sensing*, *17*(7), 1425–1432. https://doi.org/10.1080/01431169608948714

Merzlyak, M. N., Gitelson, A. A., Chivkunova, O. B., & Rakitin, V. YU. (1999). Non-destructive optical detection of pigment changes during leaf senescence and fruit ripening. *Physiologia Plantarum*, *106*(1), 135–141. https://doi.org/10.1034/j.1399-3054.1999.106119.x

Metternicht, G. (2003). Vegetation indices derived from high-resolution airborne videography for precision crop management. *International Journal of Remote Sensing*, *24*(14), 2855–2877. https://doi.org/10.1080/01431160210163074

Parida, B. R., Kushwaha, A., & Ranjan, A. K. (2022). Synergy of Sentinel-2A and Near-proximal sensor data for deriving biochemical parameters of paddy at different growth stages. *Environment, Development and Sustainability*, *24*(1), 1048–1068. https://doi.org/10.1007/s10668-021-01482-1

Pearson, R. L., & Miller, L. D. (1972). Remote mapping of standing crop biomass for estimation of the productivity of the shortgrass prairie. *Remote Sensing of Environment, VIII*, 1355.

Peng, Y., & Gitelson, A. A. (2011). Application of chlorophyll-related vegetation indices for remote estimation of maize productivity. *Agricultural and Forest Meteorology*, *151*(9), 1267–1276. https://doi.org/10.1016/j.agrformet.2011.05.005

Pinty, B., & Verstraete, M. (1992). GEMI: a non-linear index to monitor global vegetation from satellites. *Vegetatio*, *101*(1), 15–20.

Qi, J., Chehbouni, A., Huete, A. R., Kerr, Y. H., & Sorooshian, S. (1994). A modified soil adjusted vegetation index. *Remote Sensing of Environment*, *48*(2), 119–126.

Rasul, A., Balzter, H., Ibrahim, G., Hameed, H., Wheeler, J., Adamu, B., Ibrahim, S., & Najmaddin, P. (2018). Applying Built-Up and Bare-Soil Indices from Landsat 8 to Cities in Dry Climates. *Land*, *7*(3), 81. https://doi.org/10.3390/land7030081

Richardson, A. D., Braswell, B. H., Hollinger, D. Y., Jenkins, J. P., & Ollinger, S. V. (2009). Near-surface remote sensing of spatial and temporal variation in canopy phenology. *Ecological Applications*, *19*(6), 1417–1428. https://doi.org/10.1890/08-2022.1

Richardson, A. J., & Wiegand, C. (1977). Distinguishing vegetation from soil background information. *Photogrammetric Engineering and Remote Sensing*, *43*(12), 1541–1552.

Rock, B., Vogelmann, J., & Williams, D. L. (1985). Field and airborne spectral characterization of suspected damage in red spruce (picea rubens) from Vermont. *International Symposium - Machine Processing of Remotely Sensed Data*.

Rondeaux, G., Steven, M., & Baret, F. (1996). Optimization of soil-adjusted vegetation indices. *Remote Sensing of Environment*, *55*(2), 95–107.

Rouse Jr, J., Haas, R. H., Deering, D., Schell, J., & Harlan, J. C. (1974). *Monitoring the vernal advancement and retrogradation (green wave effect) of natural vegetation*.

Shingare, P. P., Hemane, P. M., & Dandekar, D. S. (2014). Fusion classification of multispectral and panchromatic image using improved decision tree algorithm. *2014 International Conference on Signal Propagation and Computer Technology (ICSPCT 2014)*, 598–603. https://doi.org/10.1109/ICSPCT.2014.6884944

Silva Junior, C. A. da, Teodoro, L. P. R., Teodoro, P. E., Baio, F. H. R., Pantaleão, A. de A., Capristo-Silva, G. F., Facco, C. U., Oliveira-Júnior, J. F. de, Shiratsuchi, L. S., Skripachev, V., Lima, M., & Nanni, M. R. (2020). Simulating multispectral MSI bandsets (Sentinel-2) from hyperspectral observations via spectroradiometer for identifying soybean cultivars. *Remote Sensing Applications: Society and Environment*, *19*, 100328. https://doi.org/10.1016/j.rsase.2020.100328

Trigg, S., & Flasse, S. (2001). An evaluation of different bi-spectral spaces for discriminating burned shrub-savannah. *International Journal of Remote Sensing*, *22*(13), 2641–2647. https://doi.org/10.1080/01431160110053185

Tucker, C. J. (1979). Red and photographic infrared linear combinations for monitoring vegetation. *Remote Sensing of Environment*, *8*(2), 127–150.

Vincini, M., Frazzi, E., & D'Alessio, P. (2008). A broad-band leaf chlorophyll vegetation index at the canopy scale. *Precision Agriculture*, *9*(5), 303–319. https://doi.org/10.1007/s11119-008-9075-z

Wang, L., & Qu, J. J. (2007). NMDI: A normalized multi-band drought index for monitoring soil and vegetation moisture with satellite remote sensing. *Geophysical Research Letters*, *34*(20), L20405. https://doi.org/10.1029/2007GL031021

Xiao, X., Boles, S., Frolking, S., Li, C., Babu, J. Y., Salas, W., & Moore, B. (2006). Mapping paddy rice agriculture in South and Southeast Asia using multi-temporal MODIS images. *Remote Sensing of Environment*, *100*(1), 95–113. https://doi.org/10.1016/j.rse.2005.10.004

Xu, H. (2008). A new index for delineating built-up land features in satellite imagery. *International Journal of Remote Sensing*, *29*(14), 4269–4276. https://doi.org/10.1080/01431160802039957

Zha, Y., Gao, J., & Ni, S. (2003). Use of normalized difference built-up index in automatically mapping urban areas from TM imagery. *International Journal of Remote Sensing*, *24*(3), 583–594. https://doi.org/10.1080/01431160304987

Zhang, N., Hong, Y., Qin, Q., & Liu, L. (2013). VSDI: A visible and shortwave infrared drought index for monitoring soil and vegetation moisture based on optical remote sensing. *International Journal of Remote Sensing*, *34*(13), 4585–4609. https://doi.org/10.1080/01431161.2013.779046

Zhao, H.-M., & Chen, X. (2005). Use of normalized difference bareness index in quickly mapping bare areas from TM/ETM+. In *International Geoscience and Remote Sensing Symposium (IGARSS)* (Vol. 3, p. 1668). https://doi.org/10.1109/IGARSS.2005.1526319